ACS ES&T Air

pubs.acs.org/estair Article

Transmission and Distribution Pipeline Leak Identification and Characterization by Walking Survey and Soil Flux Measurements

Ellis S. Robinson and Peter F. DeCarlo*

Cite This: ACS EST Air 2025, 2, 31−39 Read Online

ABSTRACT: We identified fugitive methane (CH_4) leaks within natural gas transmission and distribution pipeline rights of way (ROWs) around Pittsburgh, PA, and Baltimore, MD, by means of a walking survey while measuring ambient methane and ethane (C_2H_6) mixing ratios. We used the methane time series to determine discrete leaks using a simple algorithm and verified that the methane was fossil in origin via the methane-to-ethane ratio. For transmission ROWs, we found an average of 23 leaks (range of 12 to 47) over 20.1 total km, corresponding to an activity factor (AF) of 1.1 leaks/km (range 0.60 to 2.3 leaks/km). We also quantified total methane emissions for a subset (N = 5) of the identified leaks using a soil flux measurement chamber. The mean leak emission rate (ER) was 172 g/h/leak (range 17 to 452 g/h/leak). Our AF is higher than the Environmental Protection Agency's Greenhouse Gas Inventory (GHGI) estimate for transmission pipelines, which is 0.02 leaks/km. Our mean ER is also larger than the GHGI estimate for protected steel pipelines (44 g/h/leak). This study provides a model for making AF and ER measurements in vegetated environments with difficult terrain and suggests fugitive emissions from transmission pipelines may be a more significant source of atmospheric methane than is currently outlined in the GHGI.

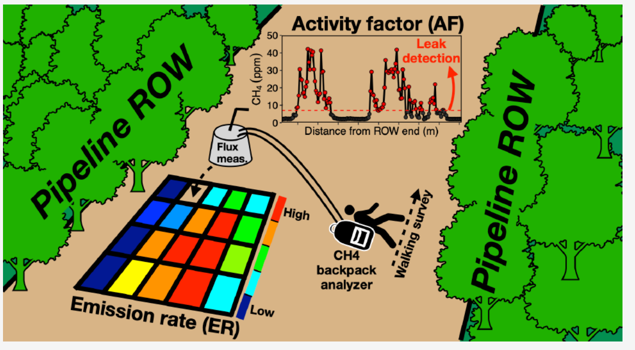

KEYWORDS: *Natural gas, transmission pipelines, fugitive methane, methane flux, leak survey*

1. INTRODUCTION

Natural gas (NG) is now the single largest source of U.S. power generation, having surpassed coal in 2016.[1] Methane (CH_4), the principal component of NG (90−95%), is a potent greenhouse gas (GHG) that contributes to atmospheric warming. Assessing the potential climate mitigation benefits of NG as a so-called "bridge fuel" replacement for coal,[2] e.g., in coal-powered electricity generation, requires quantification of the full emissions characteristics of NG over its life-cycle, from production to distribution to end-use.

Fugitive emissions from underground NG pipelines in the distribution[3,4] and gathering[5−7] sectors have been the subject of academic research in recent years in the United States. The total length of distribution and gathering pipelines has increased 36% and 60% from 1990 to 2016 (roughly 1,300,000 and 400,000 total miles in 2016, respectively), and total 2016 annual emissions for distribution and gathering pipeline leaks were 146 and 158 kt, respectively, according to the greenhouse gas inventory (GHGI) from the U.S. Environmental Protection Agency (EPA).[8] The length of U.S. transmission pipelines is similar in scale to gathering lines (roughly 300,000 total miles in 2016), but the 2016 GHGI estimate of annual fugitive emissions from transmission pipelines is only 3.3 kt, roughly 2% of the annual estimates for distribution or gathering pipelines.

The total annual emissions estimate in the GHGI for transmission pipelines is calculated from the following two quantities: the total mileage of transmission pipelines and a per-mile emissions rate (kg/mile). The annual per-mile emissions rate (ER) is 10.9 kg/mile, which has been used since 1990. The ER used in the GHGI is derived from a data set of measured leak rates of distribution pipeline leaks, not actual transmission pipeline leaks; per the GHGI, there is an assumption that distribution leaks are similar in magnitude to transmission line leaks.[9] Thus, the total annual emissions estimate for transmission pipeline fugitive emissions does not reflect, e.g., ongoing reported numbers of repaired leaks to the Pipeline and Hazardous Materials Safety Administration (PHMSA), nor is it based off of actual measured leaks from transmission pipelines.

Here we present a walking survey of ambient methane mixing ratios within both transmission and distribution pipeline rights of way (ROWs). We identified the number of

Received: May 22, 2024
Revised: December 2, 2024
Accepted: December 3, 2024
Published: December 23, 2024

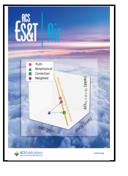

https://doi.org/10.1021/acsestair.4c00109
ACS EST Air 2025, 2, 31−39

leaks across 22.6 km of total surveyed pipeline ROWs, 20.1 km of which were transmission ROWs, and reported the leak frequency (or activity factor, AF, number of leaks per length pipeline) using different parameters. We also quantified the emissions rates for 5 of these identified leaks using detailed soil flux measurements. Our data suggest that the frequency of fugitive leaks from underground transmission lines may be underestimated and warrants further study.

2. METHODS

We conducted walking surveys of transmission and distribution pipeline ROWs in hilly, forested public lands outside of Pittsburgh, PA, and Baltimore, MD, in the late winter/early spring of 2021. Figure S1 shows a map of the study's sampling sites. We measured ground-level ambient methane and ethane mixing ratios using a Picarro Inc. GasScouter G4302 backpack instrument while walking along the nominal center of pipeline ROWs. The GasScouter is a cavity ring-down spectrometer (CRDS) that measures both methane and ethane. Picarro CRDS systems have been deployed extensively to measure NG leaks.[10−12] Ethane measurements allowed us to distinguish between fossil vs nonfossil (e.g., biogenic) methane plumes, as ethane is a component of NG but has no strong biogenic emissions sources.[13,14] Ethane-to-methane molar ratios can vary, but generally are in the range of ∼0.1−0.3 for fossil NG sources.[15,16]

2.1. Sampling Domain Description. We used the National Pipeline Mapping Service (NPMS) Public Viewer to find locations of transmission pipeline ROWs.[17] Our criteria for identifying sampling sites was simple: using the NPMS maps, we identified transmission pipeline ROWs located in public spaces (e.g., parks, state forests, etc.) where property rights would not present barriers for sampling. Distribution mains and gathering lines are explicitly not included in the NPMS, although it is possible that transmission ROWs in the NPMS could contain other pipeline types. The possibility of multiple pipelines occupying the same ROW presents a major potential confounding challenge for this study, as the locations of distribution mains and gathering lines, much less their size, depth, material, etc., are typically not found in the public domain. We will address this challenge more fully in the Discussion section. We additionally surveyed two marked pipeline ROWs (2.5 km total length) that crisscrossed the targeted transmission pipelines that were not part of the NPMS database. Given their non-inclusion within the NPMS, these ROWs do not contain transmission pipelines but instead very likely contain distribution mains (as opposed to gathering lines) and are referred to that way hereafter. Table S1 contains the full list of pipelines we surveyed, including information on location (area name and state), pipeline type (transmission or distribution), and surveyed length.

The stated spatial accuracy in the NPMS of pipeline locations is ±500 ft (∼150 m), but we determined more precise estimations of pipeline ROW locations while on-site, as ROWs in this region are typically visibly identifiable by reduced vegetation (e.g., few or no trees) and pipeline markers. Markers identifying pipeline locations are mandatory through federal law, and pipeline ROWs are required to be kept relatively clear of trees and other such debris. In all cases, we confidently identified the general locations of transmission pipeline ROWs on-site by matching locations from NPMS maps with the visual identification of marked ROWs.

Typical transmission ROWs are roughly 50 ft. wide at a minimum,[18] though pipelines may not necessarily be in the center of their ROW.[19] Therefore, 50 ft is the rough limit of our precision in determining pipeline location within an ROW. For our walking surveys, we walked nominally in the center of the ROW and in a straight path, as opposed to zig-zagging. It is possible that more leaks may have been detected using a zigzag surveying pattern simply by covering more of the ROW given our uncertainty in the exact location of the pipeline, though this would come at the expense of time and thus the ability to survey more pipeline length. Surveying in a straight path is consistent with methods employed by other mobile-platform pipeline surveys.[20−22] The GasScouter's GPS antenna records spatial coordinates at 1 hz intervals (±3 m precision) and so is not limiting in recording accuracy relative to the width of the typical ROW.

2.2. Ambient Methane Measurements. The Picarro GasScouter G4302 CRDS instrument measures optical extinction of laser light within an optical cavity bounded by two opposing mirrors, allowing for an effective path length of up to 20 km[23,24] and enabling relatively precise measurements. Full details of Picarro's CRDS measurement have been described in full elsewhere.[25] The stated precision of the GasScouter sampling at 1 Hz is 30 ppb for methane and 10 ppb for ethane. The upper limit of detection for methane is 5000 ppm.

The GasScouter flow rate is 2 L per minute. The sampling inlet for our ambient measurements consisted of 4 ft. of 1/4 in. outer diameter (1/8 in. inner diameter) Teflon tubing running from the inlet of the GasScouter down the length of a hiking pole such that the instrument sampled air at roughly 2 in. above the ground. Given the flow rate and tubing length, we estimate the residence time within the inlet tubing to less than 1 s and did not apply any spatiotemporal correction to our data. As the pole was used for walking, the height of sampling did vary on the order of a few inches with each stride, but we do not expect this to meaningfully impact our results. For comparison, the height of sampling here is considerably closer to the surface than what is typical for most vehicle-based surveys[20] and much less than UAV-based surveys.[7] Ulrich et al. show how pipeline leaks become larger areal sources as NG diffuses through soil, and so sampling as close to the surface above a leak as possible is necessary for detection in even moderately windy conditions, due both to the large (and diffuse) emissions surface as well as dispersion.[26]

The backpack form factor of the GasScouter was crucial for this study. Much of the pipeline ROWs within our sampling domain are not easily passable by a typical pickup truck or all-terrain vehicle due to stream crossings, downed trees, significant brush, and steep grades. Despite the drawback of slow speed, hiking with a backpack was the ideal surveying method for pipelines in the hilly, heavily vegetated areas of our sampling domain.

We returned to a subset of the pipelines where we identified leaks in order to verify whether these were standing leaks and to measure methane soil fluxes, as described below. In each case (N = 5), the leaks were still present after returning 3−8 weeks after the initial visit.

2.3. Leak Determination Data Analysis. Our leak determination follows a similar conceptual approach to that of Weller et al.,[27] who estimate both "leak indications" and associated emissions rates from ambient methane measurements made using a vehicle-based platform in an urban survey.

While we use a similar conceptual approach, we do not apply their framework to our data directly on account of notable differences in vehicle-based monitoring versus a walking survey. Below we detail how we used our ambient methane time series to estimate the number of leaks within the surveyed ROWs.

First, like Weller, we calculated above-background mixing ratios for both methane and ethane (ΔCH_4 and ΔC_2H_6), as background methane concentrations are subject to seasonal, diurnal, and regional variations.[28,29] We used median smoothing with sliding 20 min time intervals to calculate background mixing ratios for both species during our walking surveys. Above-background mixing ratios are the difference of the measured ambient and the calculated background mixing ratios.

To identify and count individual leaks from ambient measurements, we used an algorithmic approach based on methane threshold crossing. Briefly, we use ranges of above-background mixing ratio thresholds (ΔCH_4 = 0.5−10 ppm) and distance-windows (10−50 m) to count discrete leaks, and we report the full range of estimated leaks based on these ranges. This is conceptually very similar to Weller et al. (and also used in e.g. Maazallahi et al.[10]) in that we apply a threshold to first define a possible leak, and then consider a buffer distance that accounts for the fact that one discrete leak may be measured in multiple locations, due to meteorology and/or soil conditions.

For each ROW, we aggregated measurements at 1 m increments along its length and took the maximum above-background mixing ratio within each 1 m grid cell. The rationale for this spatial aggregation is 2-fold: first, given variable walking speeds (e.g., stopping for whatever reason, moving slowly uphill, etc.), we aim to reduce the outsized influence that certain periods have when looking at the raw time series. Second, we use physical distance as a key variable for distinguishing unique leaks from one another along the length of the pipeline. Locations along the ROW where the maximum above-background methane mixing ratio exceeded a selected threshold marked the beginning of a "leak." The end of each leak was determined by consecutive subthreshold measurements over the length of a selected distance window. A subsequent threshold crossing beyond the distance window was considered the beginning of the next leak. We considered a range of above-background methane thresholds and distance window values for leak identification. Higher threshold and longer distance-window values generally result in more conservative estimates of the number of leaks and vice versa for lower threshold and shorter distance-window values. Finding discrete leaks using above-background mixing ratio and distance-window thresholds is similar in approach to other previous surveys.[4,30,31]

Some previous studies used a single fixed threshold for defining leaks (see, e.g., Hendrick et al., who use ambient methane mixing ratios above 2.5 ppm[32]). Others use a percentage of the background value as their leak-defining threshold value, to account for temporal and spatial variations in background methane within cities[4]). Weller et al., for example, use a threshold of 110% of the background CH_4 concentration based on an analysis of detecting "leaks" from controlled-release experiments meant to simulate the context of their leak-detection study. Here, in the absence of our own controlled-release experiments, we present results based on a range of possible threshold values. Similarly, we use a range of distance windows instead of a single value. The smallest distance-window that we considered (10 m) is informed by the areal extent of the methane leaks that we measured. This value is lower than that used by Weller et al. (30 m), but again we consider a range of possible distance-windows instead of a single value and present our results as such. As shown by the above studies and which is made clear in our work as well, identifying leaks based on ambient methane measurements can vary considerably depending on these criteria. Best-practices for algorithmically determining leaks from ambient measurements specifically in walking surveys could be informed by future studies that pair blinded by-foot monitoring with underground controlled-releases, although that is outside of the scope of this work.

2.4. Soil Flux Measurements. For five of the identified leaks, we made soil flux measurements using Picarro, Inc., Soil Flux Processor (SFP), a hand-held flux-chamber attachment for the GasScouter, in order to estimate total emissions rates (ER). These leak locations are shown on Figure S1.

The SFP chamber consists of a stainless-steel, hemisphere-shaped attachment that seals with the ground. It has an outer diameter of 28 cm, a height of 15 cm, a measurement volume of 5 L, and a measurement surface area of 500 cm^2 (see photo in Figure S2b). The flux measurement works on the same principle of many other soil flux chambers, e.g., Hutchinson and Mosier,[33] where air is sampled by the instrument from within the flux chamber and recirculated back into the chamber from the outlet of the instrument through Teflon tubing.

We used Picarro SFP analysis software ("SFPLite," Picarro, Inc.) to acquire and analyze flux data. The change in methane molar concentration (mol/m^3) over time ($\Delta[CH_4]/\Delta t$) in the chamber is computed by the software, which uses measured ambient temperature and pressure in the SFP chamber and the ideal gas law to convert the volume mixing ratio (ppm) to the molar concentration. Flux (F, $mol/m^2/s$) is then determined from eq 1:

$$F = \frac{\Delta[CH_4]}{\Delta t}\frac{V}{A} \quad (1)$$

where V and A are the SFP chamber volume and cross-sectional area with the ground, respectively. We applied Hutchinson−Mosier regression fitting within SFPLite analysis software to eq 1 to quantify methane fluxes.[33]

At a given leak site, we made many individual flux measurements around the vicinity of the site where we detected elevated ambient methane. To do this systematically, we staked a grid made of webbing (46 cm × 46 cm squares in a 5 × 5 pattern, see Figure S2b) on the ground where ambient methane readings were highest. SFP chamber measurements were made in the center of each grid cell, and the grid was tessellated as necessary to continue making flux measurements until we either identified the edges of the leak or were impeded by the edge of the cleared ROW. We assume that an individual flux measurement is constant over the entire area of that grid cell; therefore, the ER for a given cell is the measured flux multiplied by the grid cell area. The sum of all grid cell ER values is the total ER that we estimate for that leak. Making a single flux measurement within a grid cell took between roughly 15 s and 3 min, and quantifying an individual leak in its entirety took roughly 3 h.

The upper detection limit (UDL) for methane in the GasScouter (5000 ppm[24]) caps the upper limit of measurable

Table 1. Summary of Results[a]

Study	Region	Pipeline type	Category	Total length (km)	AF (leaks/km)	ER (g/h/leak)	AAE (kg/km)
This study	PA and MD	Distribution	Min	2.5	2	17	3.02×10^{02}
			Mean		3.5	172	5.23×10^{03}
			Max		8.5	452	3.37×10^{04}
		Transmission	Min	20.1	0.6	17	8.90×10^{01}
			Mean		1.1	172	1.70×10^{03}
			Max		2.3	452	9.26×10^{03}
EPA GHGI, 2016[8]	Nationwide	Distribution	Total	2.07×10^{06}	0.35	214	7.10×10^{01}
			Cast Iron	4.22×10^{04}	0.38	113	7.18×10^{02}
			Unprotected steel	9.21×10^{04}	0.54	44	5.35×10^{02}
			Protected steel	7.72×10^{05}	0.15	219	6.01×10^{01}
			Plastic	1.16×10^{06}	0.01		1.79×10^{01}
		Gathering	Total	6.42×10^{05}	0.63	44	2.46×10^{02}
		Transmission	Total	4.84×10^{05}	0.02	44	6.82×10^{00}
Zimmerle et al, 2017[5]	Fayetteville shale	Gathering	Total	4.68×10^{03}			7.52×10^{02}
Lamb et al, 2015[3]	Nationwide	Distribution	Total	2.05×10^{06}	0.37	54	1.70×10^{02}
			Cast Iron	4.47×10^{04}	4.64	46	2.19×10^{03}
			Unprotected steel	9.00×10^{04}	4.04	73	1.64×10^{03}
			Protected steel	7.80×10^{05}	0.18	20	1.13×10^{02}
			Plastic	1.14×10^{06}	0.08		1.40×10^{01}
Weller et al, 2020[4]	Nationwide	Distribution	Total	2.14×10^{06}	0.82	103	8.61×10^{02}
			Cast Iron	3.22×10^{04}	1.61	134	1.46×10^{03}
			Unprotected steel	6.52×10^{04}	0.82	120	9.67×10^{02}
			Protected steel	7.71×10^{05}	0.98	122	1.03×10^{03}
			Plastic	1.27×10^{06}	0.69		7.39×10^{02}

[a]Numbers from our study in context with EPA GHGI estimates, as well as and AF and ER numbers for distribution and gathering pipelines from other studies.[3−5]

flux using the SFP; if methane in the flux chamber increases beyond the UDL too quickly, the fitting algorithm does not have enough data to use for the regression before the instrument becomes "saturated," and in these circumstances, the flux cannot be accurately quantified. We estimate 120 g/h/m^2 to be the upper-limit of methane flux that can be measured with the GasScouter and our 5-L flux chamber. This flux UDL corresponds to a ER value of 25.1 g/h over the full area of the grid cell. For instances where the methane mixing ratio in the SFP chamber increased beyond the measurement UDL too quickly for a proper flux measurement, we assign this upper-limit flux value to the measurement. This in turn means that these grid cell emissions rates are lower bound estimates. This occurred for three of the five leaks ("SC1", "MC1", and "SC2" in Figure 2) for which we present ER estimates; however, these instances only represent at most ∼5% of the total number of grid cells for these leaks.

By definition, the ER for a detected leak in our walking survey will be above the lower limit of detection (LDL) in our SFP chamber. This is because we are identifying the rough location of leaks by detecting ambient methane at above-background levels from a sampling location some small distance above the surface; the SFP chamber samples air almost directly at the surface and then serves to concentrate methane over the course of the measurement, relative to ambient air. Thus, broadly speaking, if we can detect elevated methane, we are guaranteed to be able to measure a flux at the leak site. On the level of individual grid cell measurements, we can define a LDL value for flux using the method outlined by Christiansen et al.[34] This LDL flux value is 5.9×10^{-5} g/h/m^2, using the manufacturer-stated 1 Hz precision of the GasScouter (∼30 ppb CH_4) and 120 s of sample integration time. This flux value corresponds to an ER value of 1.2×10^{-5} g/h for our grid cells. The ER value corresponding to the flux LDL is many orders of magnitude lower than the total ER for any of the leaks we measured (order 10^1 to 10^3 g/h), and still much lower than the ER for any individual grid cells that had meaningful contributions to the total ER.

We did not quantify the flux of all (or even most) identified leaks in our survey due to either time constraints and/or debris like fallen trees, shrubbery, or large stones in the vicinity of the leak. Each grid cell needed to be relatively clear of debris in order for the SFP chamber to be able to make a proper seal with the soil surface. Gaps in the emission rate (ER) maps presented in Results (Figure 2) illustrate how flux measurements were not possible in all places even for the leaks that we present estimates for, as do the logs/branches pictured in Figure S2a. These gaps, as well as the issue related to the GasScouter UDL explained above, make our total leak ER estimates necessarily lower than the bound estimates.

All data analysis and visualization was performed using open-source R programming language (v4.0.3) in RStudio software (RStudio, Inc.).[35] We used the *tidyverse*[36] (v1.3.1), *lubridate*[37] (v1.7.10), and *reshape2*[38] (v1.4.4) packages for data processing, while *ggplot2*[39] (v3.5.1) and *patchwork*[40] (v1.2.0) were used for visualization. We used *sf*[41] (v1.0.7) for all spatial analysis.

3. RESULTS

3.1. Activity Factor Determination. We sampled a total of 22.6 km of pipeline ROWs, of which 20.1 km were transmission ROWs and 2.5 km were distribution mains ROWs. Across the seven different sites where we made measurements, there were sections of 11 separate pipeline ROWs. Leaks were present in five to seven of the 11 ROWs, depending on the parameters used in our leak identification.

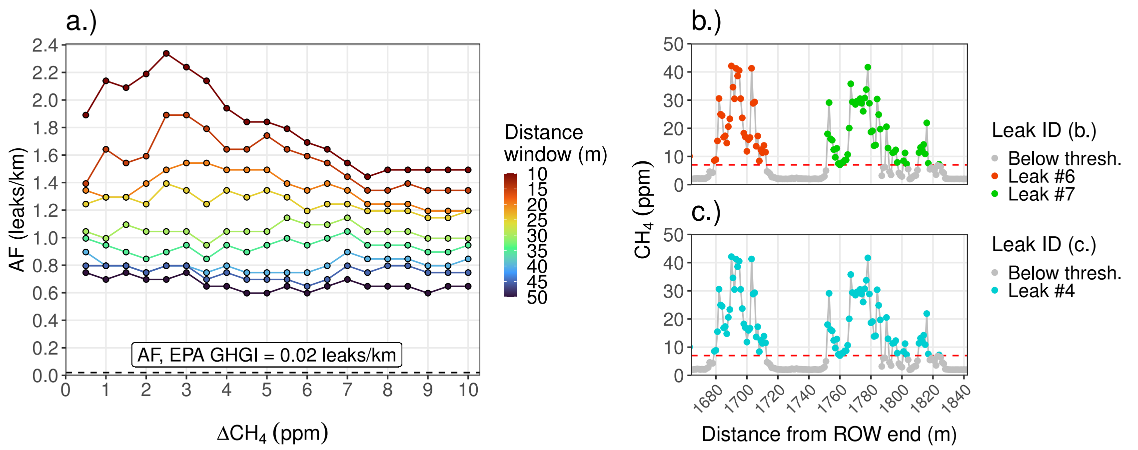

Figure 1. (a) Leak activity factor (AF) as a function of both above-baseline methane (ΔCH_4) threshold mixing ratio and distance-window values for transmission ROW data only. Panels b and c illustrate a scenario where either two (top) or one (bottom) leaks, respectively, are identified based on choice of distance-window value (40 vs 20 m, respectively) for the same ΔCH_4 threshold mixing ratio of 5 ppm.

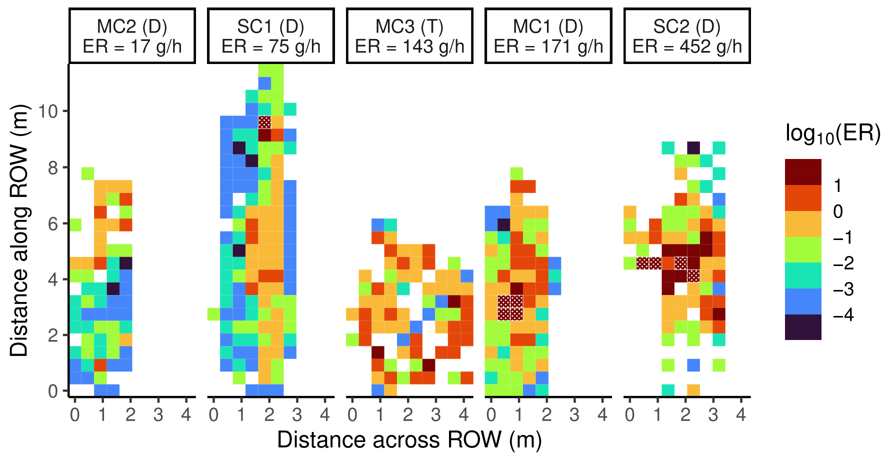

Figure 2. Spatial emissions rate (ER) maps of the five leaks quantified from the study. "SC" and "MC" refer to Settler's Cabin and Mingo Creek field sites, respectively, and "(D)" and "(T)" refer to distribution and transmission ROWs, respectively. Squares with white hatch-marks were above our detection limit, and so are assigned the UDL value, making the total ER for corresponding leaks a lower bound estimate.

The pipelines we surveyed that had at least one leak represented between 34% and 54% of the total length sampled. We found a range of 18 to 63 total methane leaks across both pipeline categories, depending on what thresholding values we used to classify leaks, with an average of 31 total leaks across all sensitivity tests.

For the distribution pipeline ROWs we sampled, we found between 5 and 21 leaks (average 9) depending on our thresholding criteria, corresponding to AF of 2–8.5 leaks/km (average 3.5 leaks/km). Notably, these AF values are similar to those reported by Lamb et al.,[3] for cast iron and unprotected steel pipelines. The transmission pipeline ROWs showed fewer leaks per km: we found between 12 and 47 total leaks (average 23) depending on thresholding criteria, corresponding to AF of 0.6–2.3 leaks/km (average 1.1 leaks/km). Table 1 summarizes our results in the context of relevant estimates of nationwide leak rates for other pipeline types (distribution and gathering) from previous studies,[3−5] as well as recent GHGI emission and activity factor estimates for transmission lines.[8] As stated in the Introduction, the GHGI uses total transmission pipeline miles and a per-mile emissions rate (kg/mile) to calculate total annual emissions from the sector. We calculated the corresponding leak frequency AF for transmission pipelines for the GHIGI listed in Table 1 using the emission factor listed for protected steel distribution mains. This assumption is reasonable given that the large majority (over 97%) of onshore transmission pipelines are protected steel.[42] Table S1 contains leak count and AF results for each of the individual pipelines we visited.

The wide range in the estimated number of methane leaks for our data set, 18–63, depends on our counting methods. Leak identification was sensitive to both the methane threshold and distance window values used, with higher thresholds and larger distance window values corresponding to fewer leaks. Figure 1a illustrates how the number of identified leaks varies for these two parameters. Figure 1b and 1c provides an anecdote that illustrates how our distance series data can result in either one or two distinct leaks being classified, depending on the distance window value used.

3.2. Emission Rate Determination. We quantified the ER for five different leaks (N = 4 for distribution ROWs and N = 1 for transmission ROWs), as shown in Figure 2. Each leak is labeled by the abbreviated field site name, leak index number, and whether the ROW was transmission or distribution (e.g., "MC1 (D)" for leak #1 at Mingo Creek site, which was in a distribution ROW). The mean ER was 172 g/h, with a wide

https://doi.org/10.1021/acsestair.4c00109
ACS EST Air 2025, 2, 31−39

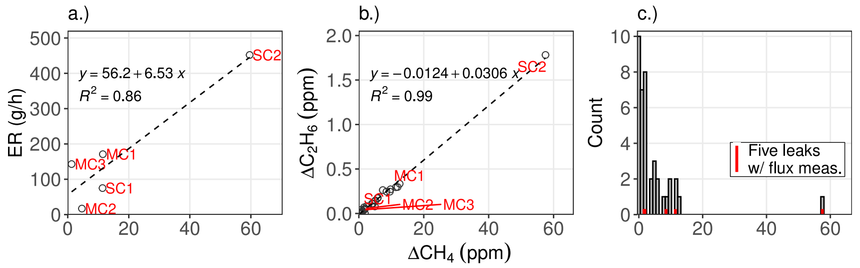

Figure 3. (a) Total leak emissions rate (ER) from soil flux measurements vs mean above-background methane mixing ratio (ΔCH_4) from walking survey data, where leaks were identified using a 20 m distance window and 0.5 ppm methane threshold. (b) Mean above-background ethane (ΔC_2H_6) vs mean above-background methane, using the same threshold values as above. The five quantified leaks are highlighted in red. (c) Histogram of mean above-background methane mixing ratios for all leaks, using the same threshold values as above. The value of the five quantified leaks are highlighted at the bottom of the plot in red.

range, from 17 to 452 g/h. Our average ER value is larger that the EPA GHGI estimate for protected steel pipeline leaks (44 g/h).

Figure 2 reveals a complicated emissions field above ground for each of the underground pipeline leaks. These maps demonstrate the challenge of fully quantifying underground pipeline leaks, as they require a large number of individual SFP measurements (range 64−131) and can often have obstacles in their midst. Quantifying each leak took multiple hours. The spatial extent of these methane leaks was on the rough order of 10 m, which informs the lower bound we chose for the distance-windows used in our leak identification. Interestingly, the largest leak by area did not have the largest total methane emissions rate.

While the focus of this paper was surveying leaks in transmission ROWs, we need to highlight that four of the five leaks for which we made soil flux measurements were in distribution ROWs. It would be more ideal if these ER measurements were all from transmission pipeline ROWs. However, the EPA GHGI ER for transmission pipeline leaks that we are comparing to is actually based on leak measurements from distribution lines and not from actual transmission lines; the magnitude of the emissions are assumed to be similar in magnitude due to more rigorous leak-detecting and repairing practices used for transmission lines.[9] Given this context, we use these five ER measurements as a single data set, though make clear which pipeline category each was made in.

Figure 3a shows each of the five measured ERs against the mean above-background methane mixing ratio from the same leak locations in the walking survey data. While there is a strong correlation (R^2 = 0.84) between ER and ΔCH_4, much of this relationship is determined by the outlier point "SC2." There appears to be little structure between ER and ΔCH_4 for the other 4 quantified leaks. It is not surprising that there may often be little correlation between ER from SFP measurements and measured ΔCH_4 from ambient walking surveys, as many variables (wind direction, wind speed, path of walker over emissions surface, etc.) can have considerable influence on measured ΔCH_4.

3.3. Supporting Evidence for Attribution to Fossil Methane Sources.

Figure 3b shows the relationship between above-background ethane and methane for all leaks identified in the walking survey for a specific threshold scenario (distance-window of 20 m and ΔCH_4 of 0.5 ppm). All instances of elevated methane that we observed had coincident elevated mixing ratios of ethane as well, giving us confidence that the methane we were measuring was of fossil origin, and the correlation between the above-background ethane and methane is quite strong (R^2 = 0.99). The slope of ambient ΔC_2H_6:ΔCH_4 is 0.031, which is similar to other studies of pipeline sources (e.g., Hopkins et al.,[15] 0.018−0.028; McKain et al.,[43] 0.024−0.027; Wennberg et al.,[16] ∼ 0.02) and is higher than other sources, such as coal beds (e.g., Ren et al.,[13] 0) or landfills (e.g., Hopkins et al.,[15] 0.01). Each of the leaks whose emission rates we quantified with SFP measurements is highlighted on the plot in red.

Other than the ethane-to-methane ratio, the fact that essentially all of the elevated methane we measured was within pipeline ROWs also gives us confidence that we are not measuring some other confounding non-pipeline natural source. Figure 4 presents a spatial analysis of above-background methane mixing ratios in each of the sampling locations in our walking survey for "Pipeline" vs "Non Pipeline" areas. Each trace is the cumulative distribution function (CDF) for measurements aggregated in 1 × 1 m grid cells that fit into each of these two land-use designations. Roughly 2.5% of grid cells in pipeline ROWs had above-background methane of at least 1 ppm, while no grid cells in the "Nonpipeline" category had correspondingly high above-background methane mixing ratios. Within the areas that we sampled, elevated methane values were essentially limited to pipeline ROWs.

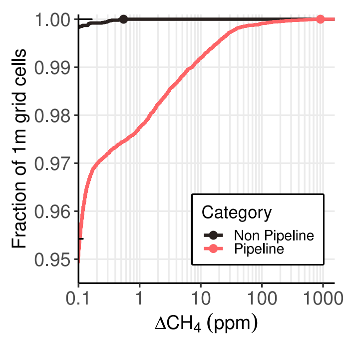

Figure 4. Cumulative distribution of mean above-background methane (ΔCH_4) mixing ratios from our walking survey, aggregated in 1 m grid cells for both pipeline and nonpipeline areas. Data over the entire survey is included. Markers at y = 1 indicate the maximum 1 Hz ΔCH_4 mixing ratio value measured within each category.

https://doi.org/10.1021/acsestair.4c00109
ACS EST Air 2025, 2, 31−39

4. DISCUSSION

There is a significant disparity between the nationwide AF estimates from the EPA GHGI and those from our walking survey of transmission pipeline ROWs, as shown in Table 1. The current EPA GHGI AF estimate for transmission lines in 0.02 leaks/km nationwide, compared to our campaign average AF of 1.10 leaks/km for pipelines in transmission ROWs. As discussed above there is a wide range in our leak estimation depending on methane threshold and distance-window values, but ven the lower bound of our estimated AF (0.60 leaks/km) is roughly 30 times greater than the EPA GHGI estimate.

We combine our AF estimates with our ER measurements to estimate total average annual emissions (AAE) per kilometer for the pipelines that we measured. The uncertainty in our AAE estimate is high given both the wide range in AF estimates and the even-wider range in ER estimates. Nonetheless, comparing per-km AAE is instructive: the lower bound of our estimate (89 kg/km) is roughly consistent with those of gathering lines and distribution lines, and much higher than transmission lines in the GHGI. The upper-bound of our per-km estimated AAE is very likely meaningless: the largest leak ("SC2") was a clear outlier in measured emissions (Figure 3a) and ambient above-background methane mixing ratio (Figure 3c). We include the full range of per-km AAE simply because we only have emissions estimates from five leaks and so do not want to throw out any of the measurements on the basis that they may be an outlier; a more detailed study would reduce the uncertainty here considerably.

We do not intend for either our AF or ER estimates to be taken as representative of transmission lines across the Mid-Atlantic region, let alone nationwide. These measurements were made in a limited geographic area at a snapshot in time (spring 2021), and represent small samples of both pipeline length (20.1 km) and number of quantified leak emissions ($N = 5$). They were mostly made in areas relatively inaccessible to vehicles and so potentially could reflect a bias compared to more-accessible transmission ROWs, though we do not know. While previous studies have reported a seasonality to fugitive NG emissions in urban pipeline networks,[44] it is not clear how any seasonal effects may be represented in our measurements. There is strong seasonality to NG consumption, with higher consumption in winter compared to summer.[45] Given that pipeline companies are required to check for transmission pipeline leaks at least annually, we speculate that the inspection schedule and inspection methods should be more impactful than any potential seasonality effect. Despite these uncertainties, there is a statistically significant difference in the leak frequency measured in our campaign compared to the EPA estimate (p-value < 0.001). It is very unlikely we would have found even our lower bound number of leaks (12 leaks) over 20.5 km of transmission pipeline by random chance, assuming that the nationwide EPA estimate applies to the pipelines we surveyed.

We speculate that the disparity between the AF we measured and that provided in the GHGI, which is based on self-reporting from industry, may depend on what qualifies a leak as "a leak." Transmission lines are required to be inspected between 1 and 4x/year (depending on class and location), a stricter requirement than for gathering and distribution lines.[46] However, the GHGI emissions estimates for the transportation pipeline sector do not appear to reflect reports of ongoing inspections or repairs.

We were unable to find any standard operating procedures from pipeline companies for inspections that used ambient methane measurements. Thus, it is hard to contextualize the threshold and distance window values that we used. From Figure 4, we see that only 0.17%, 0.1%, and 0.02% of our aggregated data had above-background methane mixing ratios above of 50, 100, and 500 ppm, respectively. This corresponds to 40, 24, and 4 total meters of pipeline, respectively. If we applied these much higher thresholds to counting leaks, we would have counted significantly fewer leaks than we did. Some thresholds may miss leaks with meaningful NG emissions, as well. For example, the smallest leak we measured ("MC1" from Figure 2, 17 g/h) would not have been counted as a leak using a threshold of 10 ppm. Another example: a 100 ppm threshold would have been too high to detect "MC3" from Figure 2 (143 g/h), and the MC3 ER is roughly double the GHGI EF.

Leak detection using ambient measurements is complicated by a variety of influences that make leak detection, much less leak emission rate determination, difficult. These include atmospheric dispersion, distance from the underground pipeline (horizontally or vertically), and dispersion characteristics of the leak through the soil.[26,47,48] Depending on the methods used by pipeline companies for detecting leaks from ambient measurement (which we do not know), it may explain the differences in our results vs. the GHGI. Indeed, the wide range in our estimated number of leaks emphasizes how sensitive leak determination is to the criteria used to define the presence of a leak. We were unable to find any threshold guidelines or operating procedures for how pipeline companies survey for leaks using ambient measurements as well as what fraction of pipelines are surveyed using ambient methane measurements vs. other methods. Pipeline companies use a range of leak detection techniques, including but not limited to measuring ambient methane.[49]

As mentioned earlier, there is a possibility that any number of the transmission pipeline ROWs we sampled may also contain pipelines of other types (e.g., distribution) which would impact the interpretation of our results as presented. If a transmission ROW where we identified leaks also contained one or more distribution mains (that were leaking), we could be misattributing identified leaks in such a case. We do not know whether or not this is true for our data set, as the locations of distribution and gathering lines are typically not found in the public domain. We can say with certainty, given their inclusion in the NPMS database, that we measured elevated methane concentrations in transmission pipeline ROWs. The existence of elevated methane within transmission pipeline ROWs does raise the question of how transmission pipeline companies would attribute leaks themselves in cases where multiple pipelines (e.g., transmission and distribution) occupy the same ROW, if they are relying on ambient measurements.

To our knowledge, these are the first reported measurements of fugitive methane leaks around transmission pipeline ROWs in the U.S. Our data show that transmission lines may potentially be a larger source of fugitive methane than is indicated by the current estimate in the EPA GHGI, albeit with a limited sample, given the much higher AF that we measured. The mean ER that we measured was also higher than the GHGI ER estimate, though within the 90% confidence interval. Our ER measurements also illustrate the spatial scale and total number of SFP measurements required to quantify total emissions from even a single underground pipeline leak in vegetated areas. To us, these results suggest that fugitive emissions from transmission pipelines are possibly an underappreciated source of methane deserving of more comprehensive study.

■ ASSOCIATED CONTENT

Supporting Information

The Supporting Information is available free of charge at https://pubs.acs.org/doi/10.1021/acsestair.4c00109.

> Additional information regarding sampling locations (Figure S1), in-field flux measurement photographs (Figure S2), and activity factor results for individual pipelines (PDF)

■ AUTHOR INFORMATION

Corresponding Author

Peter F. DeCarlo — *Department of Environmental Health and Engineering, Johns Hopkins University, Baltimore, Maryland 21218, United States;* orcid.org/0000-0001-6385-7149; Email: pdecarl1@jhu.edu

Author

Ellis S. Robinson — *Department of Environmental Health and Engineering, Johns Hopkins University, Baltimore, Maryland 21218, United States; Now at: Department of Chemical & Environmental Engineering, Tucson, Arizona 85721, United States;* orcid.org/0000-0003-1695-6392

Complete contact information is available at: https://pubs.acs.org/10.1021/acsestair.4c00109

Notes

The authors declare no competing financial interest.

■ ACKNOWLEDGMENTS

This project was self-funded and owes its existence to the Covid-19 pandemic, which postponed other projects that were previously planned. This found window of time presented the opportunity to do this field work, which is a tiny silver lining to an otherwise strange and fraught time, for which we are thankful. We also want to thank Melissa Weitz at EPA and Scot Miller at Johns Hopkins University for useful discussions about emissions data for pipelines, that helped shape the focus of our research and understanding of the emissions inventory context for these measurements. We declare no conflicts of interest for either of the authors.

■ REFERENCES

(1) U.S. Energy Information Administration. *Today in Energy: Natural Gas Expected to Surpass Coal in Mix of Fuel Used for U.S. Power Generation in 2016*, March 2016. https://www.eia.gov/todayinenergy/detail.php?id=25392# (accessed 2024-09-28).

(2) Schivley, G.; Azevedo, I.; Samaras, C. Assessing the evolution of power sector carbon intensity in the United States. *Environmental Research Letters* **2018**, *13*, 064018.

(3) Lamb, B. K.; Edburg, S. L.; Ferrara, T. W.; Howard, T.; Harrison, M. R.; Kolb, C. E.; Townsend-Small, A.; Dyck, W.; Possolo, A.; Whetstone, J. R. Direct Measurements Show Decreasing Methane Emissions from Natural Gas Local Distribution Systems in the United States. *Environ. Sci. Technol.* **2015**, *49*, 5161−5169.

(4) Weller, Z. D.; Hamburg, S. P.; von Fischer, J. C. A National Estimate of Methane Leakage from Pipeline Mains in Natural Gas Local Distribution Systems. *Environ. Sci. Technol.* **2020**, *54*, 8958−8967.

(5) Zimmerle, D. J.; Pickering, C. K.; Bell, C. S.; Heath, G. A.; Nummedal, D.; Pétron, G.; Vaughn, T. L. Gathering pipeline methane emissions in Fayetteville shale pipelines and scoping guidelines for future pipeline measurement campaigns. *Elem Sci. Anth* **2017**, *5*, 70.

(6) Li, H. Z.; Mundia-Howe, M.; Reeder, M. D.; Pekney, N. J. Constraining natural gas pipeline emissions in San Juan Basin using mobile sampling. *Science of The Total Environment* **2020**, *748*, 142490.

(7) Li, H. Z.; Mundia-Howe, M.; Reeder, M. D.; Pekney, N. J. Gathering Pipeline Methane Emissions in Utica Shale Using an Unmanned Aerial Vehicle and Ground-Based Mobile Sampling. *Atmosphere* **2020**, *11*, 716.

(8) U.S. Environmental Protection Agency. *Inventory of U.S. Greenhouse Gas Emissions and Sinks: 1990−2016, Annex 3.6*, April 2018. https://www.epa.gov/sites/production/files/2018-04/2018_ghgi_natural_gas_systems_annex_tables.xlsx (accessed 2024-09-28).

(9) U.S. Environmental Protection Agency. *Methane Emissions from the Natural Gas Industry. Volume 3: General Methodology*, June 1996. https://www.epa.gov/sites/default/files/2016-08/documents/3_generalmeth.pdf (accessed 2024-04-27).

(10) Maazallahi, H.; Fernandez, J. M.; Menoud, M.; Zavala-Araiza, D.; Weller, Z. D.; Schwietzke, S.; von Fischer, J. C.; Denier van der Gon, H.; Rockmann, T. Methane mapping, emission quantification, and attribution in two European cities: Utrecht (NL) and Hamburg (DE). *Atmospheric Chemistry and Physics* **2020**, *20*, 14717−14740.

(11) Chen, J.; Dietrich, F.; Maazallahi, H.; Forstmaier, A.; Winkler, D.; Hofmann, M. E. G.; Denier van der Gon, H.; Rockmann, T. Methane emissions from the Munich Oktoberfest. *Atmospheric Chemistry and Physics* **2020**, *20*, 3683−3696.

(12) Menoud, M.; et al. CH_4 isotopic signatures of emissions from oil and gas extraction sites in Romania. *Elementa: Science of the Anthropocene* **2022**, *10*, 1−17.

(13) Ren, X.; et al. Methane Emissions from the Marcellus Shale in Southwestern Pennsylvania and Northern West Virginia Based on Airborne Measurements. *Journal of Geophysical Research: Atmospheres* **2019**, *124*, 1862−1878.

(14) Peischl, J.; et al. Quantifying sources of methane using light alkanes in the Los Angeles basin, California. *Journal of Geophysical Research: Atmospheres* **2013**, *118*, 4974−4990.

(15) Hopkins, F. M.; Kort, E. A.; Bush, S. E.; Ehleringer, J. R.; Lai, C.; Blake, D. R.; Randerson, J. T. Spatial patterns and source attribution of urban methane in the Los Angeles Basin. *Journal of Geophysical Research: Atmospheres* **2016**, *121*, 2490−2507.

(16) Wennberg, P. O.; Mui, W.; Wunch, D.; Kort, E. A.; Blake, D. R.; Atlas, E. L.; Santoni, G. W.; Wofsy, S. C.; Diskin, G. S.; Jeong, S.; Fischer, M. L. On the Sources of Methane to the Los Angeles Atmosphere. *Environ. Sci. Technol.* **2012**, *46*, 9282−9289.

(17) National Pipeline Mapping System. *NPMS Public Viewer*. https://pvnpms.phmsa.dot.gov/PublicViewer/ (accessed: 2021-04-01).

(18) Stewart, M. *Surface Production Operations: Facility Piping and Pipeline Systems*, Vol. *III*; Gulf Professional Publishing, 2016; pp 813−884, DOI: DOI: 10.1016/b978-1-85617-808-2.00011-0.

(19) Chester County Pipeline Information Center. *Landowners Resource Guide for Pipeline Easements and Rights-of-Way*, December 2015. https://www.chescoplanning.org/pic/pdf/LandownersResourceGuide.pdf (accessed: 2024-09-28).

(20) von Fischer, J. C.; Cooley, D.; Chamberlain, S.; Gaylord, A.; Griebenow, C. J.; Hamburg, S. P.; Salo, J.; Schumacher, R.; Theobald, D.; Ham, J. Vehicle-Based Identification of Location and Magnitude of Urban Natural Gas Pipeline Leaks. *Environ. Sci. Technol.* **2017**, *51*, 4091−4099.

(21) Boothroyd, I. M.; Almond, S.; Worrall, F.; Davies, R. K.; Davies, R. J. Assessing fugitive emissions of CH4 from high-pressure gas pipelines in the UK. *Science of The Total Environment* **2018**, *631*, 1638−1648.

(22) Goetz, J. D.; Floerchinger, C.; Fortner, E. C.; Wormhoudt, J.; Massoli, P.; Knighton, W. B.; Herndon, S. C.; Kolb, C. E.; Knipping,

E.; Shaw, S. L.; DeCarlo, P. F. Atmospheric Emission Characterization of Marcellus Shale Natural Gas Development Sites. *Environ. Sci. Technol.* **2015**, *49*, 7012−7020.
(23) Picarro, Inc. *GasScouterTM G4302 Mobile Gas Concentration Analyzer*. https://www.picarro.com/environmental/products/gasscoutertm_g4302_mobile_gas_concentration_analyzer (accessed: 2024-09-28).
(24) Picarro, Inc. *Spec sheet: GasScouterTM G4302 Mobile Gas Concentration Analyzer*. https://www.picarro.com/environmental/products/gasscoutertm_g4302_mobile_gas_concentration_analyzer (accessed: 2024-09-28).
(25) Crosson, E. A cavity ring-down analyzer for measuring atmospheric levels of methane, carbon dioxide, and water vapor. *Appl. Phys. B: Laser Opt.* **2008**, *92*, 403−408.
(26) Ulrich, B. A.; Mitton, M.; Lachenmeyer, E.; Hecobian, A.; Zimmerle, D.; Smits, K. M. Natural Gas Emissions from Underground Pipelines and Implications for Leak Detection. *Environmental Science & Technology Letters* **2019**, *6*, 401−406.
(27) Weller, Z. D.; Yang, D. K.; von Fischer, J. C. An open source algorithm to detect natural gas leaks from mobile methane survey data. *PLoS One* **2019**, *14*, No. e0212287.
(28) Goetz, J. D.; Avery, A.; Werden, B.; Floerchinger, C.; Fortner, E. C.; Wormhoudt, J.; Massoli, P.; Herndon, S. C.; Kolb, C. E.; Knighton, W. B.; Peischl, J.; Warneke, C.; de Gouw, J. A.; Shaw, S. L.; DeCarlo, P. F. Analysis of local-scale background concentrations of methane and other gas-phase species in the Marcellus Shale. *Elem Sci. Anth* **2017**, *5*, 1.
(29) Metya, A.; Datye, A.; Chakraborty, S.; Tiwari, Y. K.; Sarma, D.; Bora, A.; Gogoi, N. Diurnal and seasonal variability of CO2 and CH4 concentration in a semi-urban environment of western India. *Sci. Rep.* **2021**, *11*, 2931.
(30) Gallagher, M. E.; Down, A.; Ackley, R. C.; Zhao, K.; Phillips, N.; Jackson, R. B. Natural Gas Pipeline Replacement Programs Reduce Methane Leaks and Improve Consumer Safety. *Environmental Science & Technology Letters* **2015**, *2*, 286−291.
(31) Jackson, R. B.; Down, A.; Phillips, N. G.; Ackley, R. C.; Cook, C. W.; Plata, D. L.; Zhao, K. Natural Gas Pipeline Leaks Across Washington, DC. *Environ. Sci. Technol.* **2014**, *48*, 2051−2058.
(32) Hendrick, M. F.; Ackley, R.; Sanaie-Movahed, B.; Tang, X.; Phillips, N. G. Fugitive methane emissions from leak-prone natural gas distribution infrastructure in urban environments. *Environ. Pollut.* **2016**, *213*, 710−716.
(33) Hutchinson, G. L.; Mosier, A. R. Improved Soil Cover Method for Field Measurement of Nitrous Oxide Fluxes. *Soil Science Society of America Journal* **1981**, *45*, 311−316.
(34) Christiansen, J. R.; Outhwaite, J.; Smukler, S. M. Comparison of CO2, CH4 and N2O soil-atmosphere exchange measured in static chambers with cavity ring-down spectroscopy and gas chromatography. *Agricultural and Forest Meteorology* **2015**, *211*, 48−57.
(35) RStudio Team. *RStudio: Integrated Development Environment for R*; RStudio, Inc.: Boston, MA, 2019.
(36) Wickham, H.; et al. Welcome to the tidyverse. *Journal of Open Source Software* **2019**, *4*, 1686.
(37) Grolemund, G.; Wickham, H. Dates and Times Made Easy with lubridate. *Journal of Statistical Software* **2011**, *40*, 1−25.
(38) Wickham, H. Reshaping Data with the reshape Package. *Journal of Statistical Software* **2007**, *21*, 1−20.
(39) Wickham, H. *ggplot2: Elegant Graphics for Data Analysis*; Springer Nature: New York, NY, 2016.
(40) Pedersen, T. L. *patchwork: The Composer of Plots*, R package version 1.2.0; Comprehensive R Archive Network: Vienna, 2024.
(41) Pebesma, E. Simple Features for R: Standardized Support for Spatial Vector Data. *R Journal* **2018**, *10*, 439−446.
(42) U.S. Pipeline and Hazardous Materials Safety Administration. *Gas Distribution, Gas Gathering, Gas Transmission, Hazardous Liquids, Liquefied Natural Gas (LNG), and Underground Natural Gas Storage (UNGS) Annual Report Data*. https://www.phmsa.dot.gov/data-and-statistics/pipeline/gas-distribution-gas-gathering-gas-transmission-hazardous-liquids (accessed: 2021-04-01).
(43) McKain, K.; Down, A.; Raciti, S. M.; Budney, J.; Hutyra, L. R.; Floerchinger, C.; Herndon, S. C.; Nehrkorn, T.; Zahniser, M. S.; Jackson, R. B.; Phillips, N.; Wofsy, S. C. Methane emissions from natural gas infrastructure and use in the urban region of Boston, Massachusetts. *Proc. Natl. Acad. Sci. U. S. A.* **2015**, *112*, 1941−1946.
(44) Sargent, M. R.; Floerchinger, C.; McKain, K.; Budney, J.; Gottlieb, E. W.; Hutyra, L. R.; Rudek, J.; Wofsy, S. C. Majority of US urban natural gas emissions unaccounted for in inventories. *Proc. Natl. Acad. Sci. U. S. A.* **2021**, *118*, No. e2105804118.
(45) U.S. Energy Information Administration *Today in Energy: Natural gas use features two seasonal peaks per year*, September 2015. https://www.eia.gov/todayinenergy/detail.php?id=22892# (accessed: 2024-09-28).
(46) 49 CFR 192.705 Transmission lines: Patrolling. *U.S. Code of Federal Regulations*, April 2018. https://www.govinfo.gov/content/pkg/CFR-2023-title49-vol3/pdf/CFR-2023-title49-vol3-sec192-705.pdf (accessed: 2024-09-28).
(47) Cho, Y.; Ulrich, B. A.; Zimmerle, D. J.; Smits, K. M. Estimating natural gas emissions from underground pipelines using surface concentration measurements. *Environ. Pollut.* **2020**, *267*, 115514.
(48) Jayarathne, J. R. R. N.; Zimmerle, D.; Kolodziej, R. S.; Riddick, S.; Smits, K. M. Flow and Transport of Methane from Leaking Underground Pipelines: Effects of Soil Surface Conditions and Implications for Natural Gas Leak Classification. *Environmental Science & Technology Letters* **2024**, *11*, 539−545.
(49) Korlapati, N. V. S.; Khan, F.; Noor, Q.; Mirza, S.; Vaddiraju, S. Review and analysis of pipeline leak detection methods. *Journal of Pipeline Science and Engineering* **2022**, *2*, 100074.

https://doi.org/10.1021/acsestair.4c00109
ACS EST Air 2025, 2, 31−39